

Benchmarking protocols for the metagenomic analysis of stream biofilm viromes

Meriem Bekliz¹, Jade Brandani¹, Massimo Bourquin¹, Tom Battin¹, Hannes Peter^{Corresp. 1}

¹ SBER, École Polytechnique Federale de Lausanne, Lausanne, Schweiz

Corresponding Author: Hannes Peter
Email address: hannes.peter@epfl.ch

Viruses drive microbial diversity, function and evolution and influence important biogeochemical cycles in aquatic ecosystems. Despite their relevance, we currently lack an understanding of their potential impacts on stream biofilm structure and function. This is surprising given the critical role of biofilms for stream ecosystem processes. Currently, the study of viruses in stream biofilms is hindered by the lack of an optimized protocol for their extraction, concentration and purification. Here, we evaluate a range of methods to separate viral particles from stream biofilms, and to concentrate and purify them prior to DNA extraction and metagenome sequencing. Based on epifluorescence microscopy counts of viral-like particles (VLP) and DNA yields, we optimize a protocol including treatment with tetrasodium pyrophosphate and ultra-sonication to disintegrate biofilms, tangential-flow filtration to extract and concentrate VLP, followed by ultracentrifugation in a sucrose density gradient to isolate VLP from the biofilm slurry. Viromes derived from biofilms sampled from three different streams were dominated by Siphoviridae, Myoviridae and Podoviridae and provide first insights into the viral diversity of stream biofilms. Our protocol optimization provides an important step towards a better understanding of the ecological role of viruses in stream biofilms.

1 **Benchmarking protocols for the metagenomic analysis of** 2 **stream biofilm viromes**

3 Meriem Bekliz¹, Jade Brandani¹, Massimo Bourquin¹, Tom Battin¹, Hannes Peter^{1*}

4

5 ¹ Stream Biofilm and Ecosystem Research Laboratory, Ecole Polytechnique Fédérale de
6 Lausanne, CH-1015 Lausanne, Switzerland

7

8 Corresponding Author:

9 Hannes Peter

10 Stream Biofilm and Ecosystem Research Laboratory, Ecole Polytechnique Fédérale de

11 Lausanne, CH-1015 Lausanne, Switzerland

12 Email address: Hannes.peter@epfl.ch

13

14 **Abstract**

15 Viruses drive microbial diversity, function and evolution and influence important
16 biogeochemical cycles in aquatic ecosystems. Despite their relevance, we currently lack an
17 understanding of their potential impacts on stream biofilm structure and function. This is
18 surprising given the critical role of biofilms for stream ecosystem processes. Currently, the study
19 of viruses in stream biofilms is hindered by the lack of an optimized protocol for their extraction,
20 concentration and purification.

21 Here, we evaluate a range of methods to separate viral particles from stream biofilms, and to
22 concentrate and purify them prior to DNA extraction and metagenome sequencing. Based on
23 epifluorescence microscopy counts of viral-like particles (VLP) and DNA yields, we optimize a
24 protocol including treatment with tetrasodium pyrophosphate and ultra-sonication to disintegrate
25 biofilms, tangential-flow filtration to extract and concentrate VLP, followed by

26 ultracentrifugation in a sucrose density gradient to isolate VLP from the biofilm slurry. Viromes
27 derived from biofilms sampled from three different streams were dominated by Siphoviridae,
28 Myoviridae and Podoviridae and provide first insights into the viral diversity of stream biofilms.
29 Our protocol optimization provides an important step towards a better understanding of the
30 ecological role of viruses in stream biofilms.

31

32 **Introduction**

33 Viruses are the smallest and most abundant biological entities on Earth, typically outnumbering
34 their prokaryotic and eukaryotic hosts by an order of magnitude (Rohwer, 2003, Sime-Ngando,
35 2014). Viruses are a large reservoir of genetic diversity (Suttle, 2007, Sullivan *et al.*, 2017) and
36 occur in all habitats (Paez-Espino *et al.*, 2016), including air (Reche *et al.*, 2018, Rosario *et al.*,
37 2018), soils (Srinivasiah *et al.*, 2008, Williamson *et al.*, 2017), and deep-sea sediments
38 (Danovaro *et al.*, 2008). The study of viral ecology was pioneered in surface marine systems
39 where prokaryotic viruses, also known as bacteriophages, are the main source of prokaryotic
40 mortality (Suttle, 2007, Brum and Sullivan, 2015, Gregory *et al.*, 2019) and impact ecosystem
41 functions such as the cycling of carbon (Guidi *et al.*, 2016). By lysing their hosts, horizontal gene
42 transfer and metabolic reprogramming, bacteriophages play a pivotal role in structuring
43 microbial communities (Skvortsov *et al.*, 2016, Silva *et al.*, 2017, Rossum *et al.*, 2018, Daly *et*
44 *al.*, 2019), the flow of energy and matter through food webs (Weitz *et al.*, 2015), the cycling of
45 carbon and nutrients (Dell'Anno *et al.*, 2015, Guidi *et al.*, 2016, Emerson *et al.*, 2018) and the
46 evolution of bacteria (Pal *et al.*, 2007, Rodriguez-Valera *et al.*, 2009, Simmons *et al.*, 2019).
47 Many of these strides have only recently been possible with the advent of molecular tools such as
48 metagenomic sequencing (Rosario and Breitbart, 2011, Brum and Sullivan, 2015, Roux *et al.*,
49 2016, Roux *et al.*, 2017).

50 Besides the early recognition of the potential of phages to eradicate bacterial biofilms in medical
51 settings (e.g. Chan and Abedon, 2015), little is known about the interactions between biofilms
52 and viruses (Sutherland *et al.*, 2004). While the biofilm matrix may impede the access of viruses
53 to the surface of bacterial cells (Vidakovic *et al.*, 2017), the susceptibility to phage-induced
54 clearance of biofilm has been demonstrated in laboratory experiments (Scanlan and Buckling,
55 2012). Biofilms may also act as a reservoir for virus amplification and viruses may endure
56 periods of unfavorable environmental conditions within the extracellular matrix (Doolittle *et al.*,
57 1996, Briandet *et al.*, 2008). Apart from a few examples (Dann *et al.*, 2016, Silva *et al.*, 2017,
58 Rossum *et al.*, 2018), we lack an understanding of the ecological role of viruses in streams and
59 rivers in general (Peduzzi, 2016) and in stream biofilms in particular (Battin *et al.*, 2016). In
60 streams, biofilms colonize the sedimentary surfaces of the streambed, are biodiversity hotspots
61 comprising members from all three domains of life, and fulfill critical ecosystem processes
62 (Battin *et al.*, 2016). It is reasonable therefore to speculate that viruses also control biodiversity
63 and biomass turnover in stream biofilms with potential consequences for ecosystem functioning
64 and biogeochemical cycling. However, the heterogeneous matrix of stream biofilms has
65 precluded the study of viromes in stream biofilms.

66 The first critical step towards the study of biofilm viruses in streams requires the effective
67 extraction of viral-like particles (VLPs) from the biofilm matrix. The aim of our study was
68 therefore to optimize laboratory methods for VLP extraction, concentration and purification
69 towards metagenomic analyses. Our effort was specifically tailored to maximize the yield of
70 viral DNA while minimizing DNA contamination from bacteria, eukaryotic hosts or the
71 environment. To this end, we compared a suite of sequential protocols to generate viral
72 metagenomes from stream biofilms including tangential flow filtration (TFF), polyethylene

73 glycol (PEG) precipitation, physicochemically induced biofilm breakup, and ultracentrifugation
74 followed by nucleic acid extraction. Several of these protocols have been described previously
75 (Vega Thurber et al., 2009, Danovaro and Middelboe, 2010, Hurwitz et al., 2013, Trubl et al.,
76 2016), but their rigorous testing for virome generation from stream biofilms is lacking at present.
77 We benchmark the efficiency of the different protocols using epifluorescence microscopy counts
78 of VLP and DNA yields, and provide first results of the virome structure from biofilms in three
79 streams. We provide a step-by-step version of the optimized protocol at protocols.io, which
80 allows for community participation and continuous protocol development.

81

82 **Materials & Methods**

83 **Sampling**

84 We sampled benthic biofilms from three streams (Switzerland) draining catchments differing in
85 altitude and land use (Table. 1). The Vallon de Nant (VDN) catchment is pristine with vegetation
86 dominated by alpine forests and meadows. The Veveyse (VEV) catchment is characterized by
87 mixed deciduous forests, but also agricultural and urban land use. The Senoge (SNG) catchment
88 is clearly impacted by agricultural land use. During winter, benthic biofilm were randomly
89 collected from stones (5 to 15 cm in diameter) using sterile brushes and Milli-Q water. Slurries
90 were transported on ice to the laboratory pending further processing.

91

92 **Biofilm properties**

93 For bacterial cell counting, samples were fixed with 3.7% formaldehyde (final concentration)
94 and stored at 4°C. Bacterial cells were disintegrated from the biofilm matrix using 0.25 mM
95 tetrasodium pyrophosphate in combination with rigorous shaking (1 h) and sonication (Bransonic
96 Sonifier 450, Branson) on ice (1 min). Cells were stained using Syto13 and counted on a flow

97 cytometer (NovoCyte, ACEA Biosciences); this protocol worked fine for us previously (e.g.,
98 Besemer *et al.*, 2009). Chlorophyll *a* content was determined spectrophotometrically after over-
99 night extraction in 90% EtOH (Lorenzen, 1967). Extracellular polymeric substances (EPS) were
100 extracted from biofilm slurries using 50 mM EDTA and shaking (1 h) (Battin *et al.*, 2003).
101 Carbohydrates were precipitated in 70% EtOH (-20°C, 48 h) and measured
102 spectrophotometrically as glucose equivalents (DuBois *et al.*, 1956). Proteins were determined
103 according to Lowry (Lowry *et al.*, 1951).

104

105 **Transmission electron microscopy (TEM)**

106 A first confirmation of the presence of VLP in biofilms was obtained from TEM. For this, 5 µL
107 of unprocessed sample was adsorbed to a glow-discharged carbon-coated copper grid (Canemco
108 & Marivac, Canada), washed with deionized water, and stained with 5 µL of 2% uranyl acetate.
109 TEM observations were made on an F20 electron microscope (ThermoFisher, Hillsboro, USA)
110 operated at 200 kV and equipped with a 4098 x 4098 pixel camera (CETA, ThermoFisher).
111 Magnification ranged from 10'000 to 29'000 x, using a defocus range of -1.5 to -2.5 µm.

112

113 **Protocols for the extraction of VLP**

114 We explored a variety of protocols for the concentration, extraction and purification of stream
115 biofilm VLP (Fig. 1). The concentration step is required to obtain sufficient genetic material for
116 nucleic acid extraction. Extraction aims at the liberation of VLP from the biofilm matrix, while
117 purification aims at reducing the amount of contaminant nucleic acids and cellular debris. We
118 tested all possible combinations of protocols to identify the most promising laboratory pipeline
119 for the preparation of viral metagenomes.

120 First, we homogenized the biofilm slurries by manual shaking and split samples into aliquots (1
121 L). Aliquots were centrifuged at 100 g (15 min) (5810R, Eppendorf, Hamburg, Germany) to
122 remove sediment particles and larger organisms contained within the biofilm slurry. We
123 recovered the supernatant for downstream analyses.

124

125 ***Concentration***

126 We evaluated tangential flow filtration (TFF) and polyethylene glycol (PEG) precipitation to
127 concentrate the viral size fraction. A medium-scale TFF system equipped with a 100 kDa
128 tangential flow filter (GE Healthcare, USA) was used (Vega Thurber *et al.*, 2009). Viruses were
129 collected in the retentate, whereas water and particles smaller than the pore size were discarded.
130 For each aliquot, the initial volume was reduced to less than 50 mL.

131 PEG precipitation was performed as described previously (Bibby and Peccia, 2013). Aliquot
132 biofilm samples were supplemented with 10% w/v PEG 8000 (Sigma-Aldrich, Germany) and 2.5
133 M NaCl (Sigma-Aldrich). The supernatant was then agitated by inverting the tubes three times
134 and stored overnight (4°C), followed by centrifugation for 30 minutes at 9432 g at 4°C (Sorvall
135 RC-5C centrifuge, HS-4 rotor, ThermoFisher). Supernatants were carefully removed and the
136 resulting pellets were eluted with 50 mL sterile H₂O.

137

138 ***Extraction***

139 We tested three different physicochemical treatments (chloroform, tetrasodium pyrophosphate in
140 combination with sonication and dithiothreitol (DTT)) to dislodge viruses from the biofilm
141 matrix. The order - first volume reduction, then chemical detachment - was chosen because the
142 chemicals used for extraction of VLPs may damage TFF filters.

143 To one subset of the samples, we added 0.2 volumes of chloroform and mixed by inversion.
144 Then, these samples were incubated at 4°C for 30 minutes, vortexed every 5 minutes, and
145 centrifuged at 3234 g for 15 minutes at 4° C (5810R, Eppendorf, Germany) to recover the
146 supernatant (Marhaver *et al.*, 2008, Vega Thurber *et al.*, 2008).

147 Following the recommendation of Danovaro and Middelboe (2010), we used sonication in
148 combination with tetrasodium phosphate to separate viruses from biofilms. For this, we added 5
149 mM of tetrasodium pyrophosphate (final concentration) to another subset of concentrated biofilm
150 samples and incubated them in the dark (15 minutes). Then, all samples were sonicated
151 (frequency: 40 KHz; Branson Sonifier 450, Branson) three times for 1 minute with 30-second
152 intervals during which the samples were manually shaken. To prevent heating, samples were put
153 on ice during sonication. Finally, one subset of the samples were treated with 6.5 mM DTT and
154 incubated for 1 hour at 37°C. At the end of the incubation period, samples were chilled on ice.

155 Biofilm samples without chemical treatment served as controls. After each treatment, these
156 samples were first centrifuged (4°C) at 3'234 g for 15 minutes (5810R, Eppendorf) and the
157 supernatant was sequentially filtered through 0.8 µm and 0.45 µm filters (Whatman, GE
158 Healthcare, USA) to remove debris and cells.

159

160 ***Purification***

161 To eliminate contaminating eukaryotic, prokaryotic and extracellular nucleic acids, DNase I at a
162 final concentration of 2.5U/µL (Life Technologies, Germany) and Tris buffer (100 mM Tris pH
163 7.5, 5 mM CaCl₂ and 25 mM MgCl₂) were added to the clarified supernatant and incubated at
164 37°C (2 h). To confirm the removal of contaminant DNA, polymerase chain reaction (PCR)
165 targeting the 16S rRNA gene was performed using the universal primer pair 341f (5'-

166 CCTACGGGNGGCWGCAG-3') and 785r (5'-GACTACHVGGGTATCTAAKCC-3'). PCR
167 amplification was performed with a Biometra Thermal Cycler using Taq ALLin polymerase
168 (Axon Lab) according to the manufacturer's instructions with an initial enzyme activation step
169 (95°C for 2 minutes) followed by 30 cycles of denaturation (95°C for 30 seconds) and
170 hybridization (72°C for 30 seconds) and a final elongation (72°C for 10 minutes). PCR products
171 were visualized under UV light after migration on an agarose gel stained using GelRed (Biotium,
172 USA).

173 For final purification of the viral DNA fraction, two protocols of density gradient
174 ultracentrifugation were assessed. A subset of sample was deposited on top of a CsCl gradient
175 composed of layers of 1 mL of 1.7, 1.5, 1.35 and 1.2 g/mL CsCl, and centrifuged at 106'800 g
176 (Optima XPN-80 Ultracentrifuge, 32 SWi, Beckman Coulter, USA) for 2 h (4°C). The viral
177 fraction was harvested from the interface between the 1.5 and 1.7 g/mL CsCl layers using an
178 18G needle. Similarly, sucrose gradient ultracentrifugation was assessed for final purification of
179 the viral fraction. The sucrose gradient consisted of 3 mL of 0.2- μ m filtered 66% sucrose and 7
180 mL of 0.2- μ m filtered 30% sucrose. The viral fraction was harvested from the interface between
181 both layers using an 18G needle.

182

183 **Enumerating VLPs using epifluorescence microscopy**

184 To assess the relative viral extraction efficiency of the various protocols, we counted VLP under
185 an epifluorescence microscopy (AxioImager Z2, Zeiss, Germany) as described by Patel et al.
186 (2007). Because of high background noise owing to the biofilm matrix constituents, samples
187 could only be counted after the purification steps. Subsamples were fixed with formaldehyde,
188 stained with SYBR gold (Molecular Probes, ThermoScientific, USA) and incubated at room

189 temperature in the dark (30 minutes). After incubation, each sample was filtered onto a 0.02 μm
190 pore size membrane filter (Anodisc, Whatman). The filters were mounted on glass slides with a
191 drop of VECTASHIELD antifade mounting medium (Vector Laboratories, Burlingame, USA).
192 VLP were visualized using blue light (488 nm) excitation and green (512 nm) emission. For each
193 sample, 15 to 20 randomly selected images were acquired with a camera (AxioCam 506 mono,
194 Zeiss) mounted onto the microscope. VLPs were discriminated from bacteria by size (0.015 to
195 0.2 μm) and enumerated using a custom script in Fiji (Schindelin *et al.*, 2012).

196

197 **Nucleic acid extraction**

198 To further assess the efficiency of the tested protocols to obtain viral nucleic acids for
199 metagenome sequencing, we extracted DNA and quantified its concentration. Following
200 Sambrook *et al.* (1989), purified viral samples were suspended in 0.1 volume of TE buffer, 0.01
201 volume of 0.5 M EDTA (pH 8) and 1 volume of formamide, and incubated at room temperature
202 (30 minutes). Then, two volumes of 100% EtOH were added and incubated 30 minutes (4°C).
203 Samples were centrifuged at 17'000 g (4°C, 20 minutes) and pellets washed twice with 70% cold
204 EtOH. Pellets were air-dried and resuspended in 567 μL of TE buffer (10 mM Tris and 1 mM
205 EDTA (pH 8.0)). Thirty μL of warm 10% SDS and 3 μL of proteinase K (20 mg/mL) were
206 added and samples were incubated for 1 h at 37°C. Next, 100 μL of 5M NaCl and 80 μL of
207 warm CTAB were added and incubated for 10 minutes (65°C). DNA was extracted in a series of
208 chloroform, phenol:chloroform:isoamyl alcohol (25:24:1) and chloroform treatments, with
209 centrifugation at 16'000 g (10 minutes) for phase separation. Finally, DNA was precipitated
210 overnight in isopropanol (-20°C). DNA was concentrated by centrifugation at 16'000 g (4°C)
211 for 20 min, and the pellet washed twice with cold 70% EtOH, air-dried, resuspended in 50 μL

212 nuclease-free H₂O and stored (−20°C). DNA concentration was measured using Qubit and the
213 dsDNA high-sensitivity kit according to the manufacturer's instructions (Life Technologies,
214 Carlsbad, USA).

215

216 **Library construction and sequencing**

217 Based on the epifluorescence microscopy counts of VLP and the DNA concentration from
218 purified biofilm samples, we selected samples processed with the best performing pipeline for
219 metagenome sequencing. For sequencing library construction, DNA was sheared with an S2
220 focused ultrasonicator (Covaris, Woburn, USA) to achieve a target size of DNA fragments of
221 around 350 bp. We opted for the ACCEL-NGS® 1S PLUS DNA library kit (Swift Biosciences,
222 USA) which allows low quantities of both single- and double-stranded DNA as input (Roux *et*
223 *al.*, 2016). Library construction and multiplexing was performed following the manufacturer's
224 instructions for DNA inputs (<1 ng/μL) and 20 cycles of indexing PCR. Paired-end sequencing
225 (2 x 300 bp) was performed on a MiSeq System (Illumina, San Diego, USA) at the Lausanne
226 Genomic Technologies Facilities. Raw sequences have been submitted to the European
227 Nucleotide Archive under accession number PRJEB33548.

228

229 **Bioinformatic analyses**

230 The number of reads and GC content of each sample before and after quality control were
231 calculated using a custom python script. For virome classification, we followed the
232 recommendations to assemble viral contiguous sequences (contigs) according to Roux *et al.*
233 (2019). First, BBDuk (v35.79) was used to remove Illumina adapters, filtering and trimming
234 (trimq=12). Next, reads with >93% similarity to a human reference genome were discarded

235 (using BBmap). The ACCEL-NGS[®] 1S Plus library preparation kit includes a low complexity
236 adaptase tail, which was clipped (10 bases) according to the manufacturer's instructions. We
237 then used the error correction capability of Tadpole (v. 37.76) to correct for sequencing errors
238 (mode=correct ecc=t prefilter=2). Prior to assembly, we de-duplicated our datasets using
239 clumpify (v37.76) with parameters set such that identical reads were identified and only one
240 copy was retained (dedupe subs=0). Finally, we used the SPAdes assembler (v3.13.0, Bankevich
241 *et al.*, 2012) in single-cell (--sc) mode, with error correction disabled (--only-assembler) and
242 kmers set to 21, 33, 55, 77, 99, 127 to assemble contigs. We co-assembled the paired-end reads
243 from both sequencing runs for each sample individually. To obtain an overview of the potential
244 contaminant sequences (e.g., human, bacterial and phiX), we uploaded the quality-trimmed and
245 de-replicated reads (forward orientation only) to the web interface of taxonomer (Flygare *et al.*,
246 2016). Taxonomer is an ultrafast taxonomy assigner, which assigns and classifies reads to
247 human, bacterial, viral, phage, fungal, phix, ambiguous (i.e., reads fit to more than one bin) and
248 "unknown" bins. For identification and classification of viral contigs, we used MetaPhinder
249 (v2.1, Jurtz *et al.*, 2016) through the web interface hosted at the Center for Genomic
250 Epidemiology at the Danish Technical University (DTU). Additionally, we queried the Viral_rep
251 and Phage_F domains of the PFAM database using hmmsearch (HMMER v3, Eddy, 2011) to
252 identify ssDNA contigs (Trubl *et al.*, 2019).

253

254 **Results**

255 **Biofilm properties**

256 Bacterial abundance ranged between 4.1×10^{11} cells m⁻² at the lowest stream (SNG) and $2.3 \times$
257 10^9 cells m⁻² at the uppermost stream (VDN; Table 1). This pattern was mirrored by an increase
258 in chlorophyll *a* content, and the protein and carbohydrate concentrations in EPS that were

259 higher in the lowland than the high-altitude stream (Table 1). Despite these differences in biofilm
260 properties, no differences in extraction efficiency among the different protocols were detected. In
261 fact, the average number of VLPs extracted by the various protocols were strongly correlated
262 among the different samples (pairwise Spearman's r_s ranging between 0.94 and 0.98).

263

264 **Transmission Electron Microscopy (TEM)**

265 Direct electron microscopic observations of raw biofilm samples revealed the presence and
266 morphological diversity of virions, including tailed bacteriophages and lemon-shaped viruses, in
267 biofilms from all three streams (Fig. 2). Polyhedral, spherical and filamentous VLPs were also
268 observed, which may include untailed bacteriophages or viruses infecting eukaryotes.

269

270 **Virome extraction and purification**

271 In total, we evaluated 16 protocols to concentrate, extract and purify viruses from benthic
272 biofilms from three streams (Fig. 1). Based on the number of VLPs and DNA yields retained at
273 the end of each protocol, we observed significant differences in relative extraction efficiencies
274 among protocols. Across all samples, average VLP counts and DNA yields were correlated
275 (Spearman's $r_s = 0.74$), suggesting conformity among these two means of evaluation. The
276 combination of TFF for concentration, tetrasodium pyrophosphate and sonication for extraction,
277 and sucrose gradient centrifugation for purification resulted in the highest VLP counts in all three
278 samples (two-way ANOVA, $p < 0.01$; Fig. 3). This pipeline also yielded highest DNA
279 concentration (Fig. 4). Protocols involving PEG precipitation generally resulted in a lower
280 recovery of VLPs (on average only 13.6 % compared to the best performing pipeline) and DNA
281 yields below detection limit. This may be attributable to the formation of a visible, viscous layer

282 upon addition of PEG to the biofilm samples. The dissociation of VLPs from the biofilm matrix
283 was most effective using tetrasodium pyrophosphate and sonication (two-way ANOVA, $p < 0.01$).
284 Protocols based on TFF and using DTT or chloroform extracted on average 25.0% and 33.2%
285 less VLPs than protocols using TFF followed by tetrasodium pyrophosphate treatment and
286 sonication (Fig. 3). Samples without any physicochemical treatment to extract VLP from
287 biofilms yielded on average 54.8% less VLPs than the tetrasodium pyrophosphate and sonication
288 treatment. To further purify viruses, two discontinuous gradient formulations with sucrose and
289 CsCl were tested. On average, 1.9 times more VLPs were retained by ultracentrifugation using
290 the sucrose gradient than using the CsCl gradient in samples concentrated using TFF and treated
291 with tetrasodium pyrophosphate and sonication (paired-T-Test, $p < 0.01$). This is also reflected in
292 DNA yields, which reached $1.22 \text{ ng } \mu\text{L}^{-1}$ in VDN, $1.31 \text{ ng } \mu\text{L}^{-1}$ in VEV and $18.7 \text{ ng } \mu\text{L}^{-1}$ in SNG
293 using TFF, pyrophosphate and sonication followed by sucrose gradient centrifugation. DNA
294 yields were on average 3 times higher using ultracentrifugation in the sucrose compared to the
295 CsCl gradient (paired T-Test, $p = 0.03$) and on average 1.5, 1.7 and 1.9 times higher using
296 tetrasodium pyrophosphate and sonication compared to DTT, no physico-chemical detachment
297 and chloroform, respectively.

298 Given that stream biofilms contain abundant prokaryotic, eukaryotic and extracellular DNA, it is
299 crucial to verify the absence of DNA potentially contaminating the samples. Negative PCR
300 results from samples treated with DNase I confirmed the absence of DNA contamination from
301 prokaryotic cells.

302

303 **Stream biofilm viromes**

304 From the two sequencing runs we obtained 24'388'096, 22'459'218 and 23'804'190 paired-end
305 reads from SNG, VEV and VDN, respectively (Table 2). After quality control, error correction
306 and deduplication, on average 97.5% of the reads remained. Initial screening using taxonomer
307 showed that human contaminant reads accounted for 0.13 to 0.25% of the reads, while bacterial
308 contaminant reads accounted for 1.47 to 8.11% of the reads.

309 We obtained 3698, 11'323 and 13'591 contigs from de-novo assembly of quality-controlled and
310 deduplicated reads from SNG, VEV and VDN, respectively. The largest contigs were 9493,
311 46'665 and 54'492 bp in SNG, VEV and VDN, respectively. Hmsearch against the PFAM
312 databases did not yield ssDNA contigs in the three viromes. Between 726 and 2613 contigs were
313 classified as of viral origin in the three viromes (Fig. 5). In all samples, the majority of contigs
314 were identified as not further classified Siphoviridae (28.3 – 53.3%), followed by Myoviridae
315 (9.6 – 18.0%) and Podoviridae (4.7 – 5.2%). Contigs classified as T4virus, Cp220virus, Kayvirus
316 and P12024virus were common in all three biofilm viromes. However, contigs classified as
317 Twortvirus, Phicbkvirus, Coopervirus and L5virus were only detected in viromes obtained from
318 VEV and VDN but not in SNG.

319

320 Discussion

321 The advent of metagenomic tools has revolutionized the study of the role of viruses in numerous
322 ecosystems (Suttle, 2007, Rosario and Breitbart, 2011, Brum and Sullivan, 2015, Trubl *et al.*,
323 2019). For biofilms in general, and particularly for biofilms in streams and rivers, however, an
324 optimized protocol for viral metagenomics has been missing. Here, we establish an optimized
325 sample-to-sequence pipeline for the concentration and purification of viruses from stream
326 biofilms. This protocol is publicly available at [https://www.protocols.io/view/extraction-and-](https://www.protocols.io/view/extraction-and-purification-of-viruses-from-stream-32qqdw)
327 [purification-of-viruses-from-stream-32qqdw](https://www.protocols.io/view/extraction-and-purification-of-viruses-from-stream-32qqdw). We used two metrics, the number of VLP retained

328 and the amount of DNA extracted from the samples to evaluate the performance of the different
329 combinations of protocols (Fig. 3, Fig. 4). This approach allowed us to obtain a relative
330 comparison among the tested protocols. However, it does not permit the quantification of
331 extraction efficiencies since it was not possible to enumerate VLPs without prior extraction and
332 purification.

333 The best performing sample-to-sequence pipeline involves TFF for sample concentration,
334 pyrophosphate and sonication for the detachment of viruses from the biofilm matrix and DNase I
335 treatment followed by sucrose gradient ultracentrifugation for purification. This is similar to
336 protocols for other complex samples, such as soils (Trubl *et al.*, 2016) or marine and freshwater
337 sediments (Danovaro and Middelboe, 2010). The suggested combination of protocols was
338 consistently the best performing pipeline for biofilms obtained from three streams differing in
339 trophic state and with different biofilm properties (Table 1).

340 The viromes obtained using the best-performing protocol were dominated by reads of viral or
341 unknown origin (presumably reflecting the lack of viral sequences in public databases), and
342 contaminant sequences (i.e., of bacterial or human origin) contributed only marginally to the
343 viromes. Following an optimized assembly strategy (Roux *et al.*, 2019), the reads assembled into
344 a large number of contigs, however, of small average contig size. Still many of the contigs were
345 classified as of viral origin. Viral community composition was remarkably similar across the
346 three different stream biofilms, with several contigs classified as T4virus, Cp220virus, Kayvirus
347 and P12024virus found in all samples. Despite the use of the ACCEL-NGS® 1S PLUS DNA kit
348 (Roux *et al.*, 2016), ssDNA viruses, which account for <5% of DNA viral communities in other
349 freshwater, marine and soil ecosystems (Roux *et al.*, 2016, Trubl *et al.*, 2019) could not be
350 detected in the viromes from stream biofilms. Strikingly, the virome obtained from the most

351 eutrophic stream (SNG) resulted in the lowest number of viral contigs and lacked contigs
352 classified as Twortvirus, Phicbkvirus, Coopervirus and L5virus. However, given the low number
353 of samples, we caution against concluding an anthropogenic effect on stream biofilm viral
354 communities.

355 A range of chemical properties may explain the relative differences in virus extraction efficiency
356 from stream biofilms. PEG precipitation generally failed to concentrate viruses from biofilm
357 slurries, potentially due to the formation of a viscous layer that impaired PEG removal.
358 Previously described methods for isolating viruses involve chloroform (Marhaver *et al.*, 2008,
359 Vega Thurber *et al.*, 2008, Hewson *et al.*, 2012); however, chloroform may denature the lipid
360 envelopes surrounding viral capsids, internal lipid membranes and nucleo-cytoplasmic large
361 DNA viruses (NCLDV), including Phycodnaviridae, which predominantly infect freshwater and
362 marine algae, may be sensitive to chloroform treatment (Feldman and Wang, 1961). Moreover,
363 ssDNA viruses lack a lipid envelope and some tailed bacteriophages may display sensitivity to
364 chloroform. Similarly, DTT is a reducing agent, which breaks disulfide bonds in proteins. This
365 may explain to the reduced recovery of VLPs from samples treated with PEG, chloroform or
366 DTT.

367 Extracellular DNA is a common component of the biofilm matrix (Flemming and Wingender,
368 2010), which together with DNA from damaged eukaryotic and prokaryotic cells needs to be
369 removed prior to virome sequencing. We propose a DNase I treatment as an efficient way to
370 digest extracellular DNA from biofilms, followed by sucrose density gradient ultracentrifugation
371 for further purification. This order is important because otherwise DNA from viral particles
372 damaged during ultracentrifugation may be digested by the DNase digestion. Compared to
373 ultracentrifugation in a CsCl gradient, sucrose gradient ultracentrifugation probably maximized

374 the purification of a wider range of viruses because of the larger gradient of densities recovered
375 with this method. Moreover, CsCl density gradient separation may exclude viral particles as that
376 may be too buoyant (Vega Thurber *et al.*, 2009), or degrade the structure of enveloped viruses
377 (Lawrence and Steward, 2010) and therefore reduce their recovery. A critical step of virome
378 preparation concerns the nucleic acid extraction. We chose a derivation of a standard protocol,
379 which allows the extraction of both ssDNA and dsDNA viruses (Sambrook *et al.*, 1989).

380

381 **Conclusions**

382 In conclusion, we provide a first protocol for the generation of viromes from stream biofilms.
383 This paves the way for a better understanding of the roles viruses may play in stream ecology.
384 By providing a step-by-step protocol on protocols.io, we hope to further stimulate research on
385 phage diversity in stream biofilms.

386

387 **Acknowledgements**

388 We acknowledge the help of Davide Demurtas for TEM imaging.

389

390 **References**

- 391 Bankevich A, Nurk S, Antipov D, Gurevich AA, Dvorkin M, Kulikov AS *et al.* (2012). SPAdes:
392 a new genome assembly algorithm and its applications to single-cell sequencing. *J*
393 *Comput Biol* **19**: 455-477.
- 394 Battin TJ, Kaplan LA, Newbold JD, Cheng X, Hansen C (2003). Effects of current velocity on
395 the nascent architecture of stream microbial biofilms. *Appl Environ Microbiol* **69**: 5443-
396 5452.
- 397 Battin TJ, Besemer K, Bengtsson MM, Romani AM, Packmann AI (2016). The ecology and
398 biogeochemistry of stream biofilms. *Nat Rev Microbiol* **14**: 251-263.
- 399 Besemer K, Singer G, Hödl I, Battin TJ (2009). Bacterial Community Composition of Stream
400 Biofilms in Spatially Variable-Flow Environments. *Applied and Environmental*
401 *Microbiology* **75**: 7189.
- 402 Bibby K, Peccia J (2013). Identification of viral pathogen diversity in sewage sludge by
403 metagenome analysis. *Environ Sci Technol* **47**: 1945-1951.

- 404 Briandet R, Lacroix-Gueu P, Renault M, Lecart S, Meylheuc T, Bidnenko E *et al.* (2008).
405 Fluorescence correlation spectroscopy to study diffusion and reaction of bacteriophages
406 inside biofilms. *Appl Environ Microbiol* **74**: 2135-2143.
- 407 Brum JR, Sullivan MB (2015). Rising to the challenge: accelerated pace of discovery transforms
408 marine virology. *Nature Reviews Microbiology* **13**: 147.
- 409 Chan BK, Abedon ST (2015). Bacteriophages and their enzymes in biofilm control. *Curr Pharm*
410 *Des* **21**: 85-99.
- 411 Daly RA, Roux S, Borton MA, Morgan DM, Johnston MD, Booker AE *et al.* (2019). Viruses
412 control dominant bacteria colonizing the terrestrial deep biosphere after hydraulic
413 fracturing. *Nat Microbiol* **4**: 352-361.
- 414 Dann LM, Paterson JS, Newton K, Oliver R, Mitchell JG (2016). Distributions of Virus-Like
415 Particles and Prokaryotes within Microenvironments. *PLoS One* **11**: e0146984.
- 416 Danovaro R, Dell'Anno A, Corinaldesi C, Magagnini M, Noble R, Tamburini C *et al.* (2008).
417 Major viral impact on the functioning of benthic deep-sea ecosystems. *Nature* **454**: 1084.
- 418 Danovaro R, Middelboe M (2010). Separation of free virus particles from sediments in aquatic
419 systems. In: Wilhelm SW, Weinbauer MG, Suttle CA (eds). *Manual of Aquatic Viral*
420 *Ecology*. . American Society of Limnology and Oceanography: Waco, TX.
- 421 Dell'Anno A, Corinaldesi C, Danovaro R (2015). Virus decomposition provides an important
422 contribution to benthic deep-sea ecosystem functioning. *Proc Natl Acad Sci U S A* **112**:
423 E2014-2019.
- 424 Doolittle MM, Cooney JJ, Caldwell DE (1996). Tracing the interaction of bacteriophage with
425 bacterial biofilms using fluorescent and chromogenic probes. *J Ind Microbiol* **16**: 331-
426 341.
- 427 DuBois M, Gilles KA, Hamilton JK, Rebers PA, Smith F (1956). Colorimetric Method for
428 Determination of Sugars and Related Substances. *Analytical Chemistry* **28**: 350-356.
- 429 Eddy SR (2011). Accelerated Profile HMM Searches. *PLoS Comput Biol* **7**: e1002195.
- 430 Emerson JB, Roux S, Brum JR, Bolduc B, Woodcroft BJ, Jang HB *et al.* (2018). Host-linked soil
431 viral ecology along a permafrost thaw gradient. *Nature Microbiology* **3**: 870-880.
- 432 Feldman HA, Wang SS (1961). Sensitivity of Various Viruses to Chloroform. *Proceedings of the*
433 *Society for Experimental Biology and Medicine* **106**: 736-738.
- 434 Flemming HC, Wingender J (2010). The biofilm matrix. *Nat Rev Microbiol* **8**: 623-633.
- 435 Flygare S, Simmon K, Miller C, Qiao Y, Kennedy B, Di Sera T *et al.* (2016). Taxonomer: an
436 interactive metagenomics analysis portal for universal pathogen detection and host
437 mRNA expression profiling. *Genome Biol* **17**: 111.
- 438 Gregory AC, Zayed AA, Conceicao-Neto N, Temperton B, Bolduc B, Alberti A *et al.* (2019).
439 Marine DNA Viral Macro- and Microdiversity from Pole to Pole. *Cell* **177**: 1109-1123
440 e1114.
- 441 Guidi L, Chaffron S, Bittner L, Eveillard D, Larhlimi A, Roux S *et al.* (2016). Plankton networks
442 driving carbon export in the oligotrophic ocean. *Nature* **532**: 465-470.

- 443 Hewson I, Brown JM, Burge CA, Couch CS, LaBarre BA, Mouchka ME *et al.* (2012).
444 Description of viral assemblages associated with the *Gorgonia ventalina* holobiont. *Coral*
445 *Reefs* **31**: 487-491.
- 446 Hurwitz BL, Deng L, Poulos BT, Sullivan MB (2013). Evaluation of methods to concentrate and
447 purify ocean virus communities through comparative, replicated metagenomics. *Environ*
448 *Microbiol* **15**: 1428-1440.
- 449 Jurtz VI, Villarroel J, Lund O, Voldby Larsen M, Nielsen M (2016). MetaPhinder-Identifying
450 Bacteriophage Sequences in Metagenomic Data Sets. *PLoS One* **11**: e0163111.
- 451 Lawrence JE, Steward GF (2010). Purification of viruses by centrifugation. In: Wilhelm SW,
452 Weinbauer MG, Suttle CA (eds). *Manual of Aquatic Viral Ecology*. ASLO. pp 166–181.
- 453 Lorenzen CJ (1967). Determination of chlorophyll and pheo-pigments: spectrophotometric
454 equations. *Limnology and Oceanography* **12**: 343-346.
- 455 Lowry OH, Rosebrough NJ, Farr AL, Randall RJ (1951). Protein measurement with the Folin
456 phenol reagent. *The Journal of biological chemistry* **193**: 265-275.
- 457 Marhaver KL, Edwards RA, Rohwer F (2008). Viral communities associated with healthy and
458 bleaching corals. *Environmental microbiology* **10**: 2277-2286.
- 459 Paez-Espino D, Eloie-Fadrosh EA, Pavlopoulos GA, Thomas AD, Huntemann M, Mikhailova N
460 *et al.* (2016). Uncovering Earth's virome. *Nature* **536**: 425-430.
- 461 Pal C, Macia MD, Oliver A, Schachar I, Buckling A (2007). Coevolution with viruses drives the
462 evolution of bacterial mutation rates. *Nature* **450**: 1079-1081.
- 463 Patel A, Noble RT, Steele JA, Schwalbach MS, Hewson I, Fuhrman JA (2007). Virus and
464 prokaryote enumeration from planktonic aquatic environments by epifluorescence
465 microscopy with SYBR Green I. *Nat Protoc* **2**: 269-276.
- 466 Peduzzi P (2016). Virus ecology of fluvial systems: a blank spot on the map? *Biol Rev Camb*
467 *Philos Soc* **91**: 937-949.
- 468 Reche I, D'Orta G, Mladenov N, Winget DM, Suttle CA (2018). Deposition rates of viruses and
469 bacteria above the atmospheric boundary layer. *ISME J* **12**: 1154-1162.
- 470 Rodriguez-Valera F, Martin-Cuadrado A-B, Rodriguez-Brito B, Pasic L, Thingstad TF, Rohwer
471 F *et al.* (2009). Explaining microbial population genomics through phage predation.
472 *Nature Reviews Microbiology* **7**: 828-836.
- 473 Rohwer F (2003). Global Phage Diversity. *Cell* **113**: 141.
- 474 Rosario K, Breitbart M (2011). Exploring the viral world through metagenomics. *Curr Opin*
475 *Virol* **1**: 289-297.
- 476 Rosario K, Fierer N, Miller S, Luongo J, Breitbart M (2018). Diversity of DNA and RNA
477 Viruses in Indoor Air As Assessed via Metagenomic Sequencing. *Environ Sci Technol*
478 **52**: 1014-1027.
- 479 Rossum TV, Uyaguari-Diaz MI, Vlok M, Peabody MA, Tian A, Cronin KI *et al.* (2018).
480 Spatiotemporal dynamics of river viruses, bacteria and microeukaryotes. *bioRxiv*:
481 259861.

- 482 Roux S, Solonenko NE, Dang VT, Poulos BT, Schwenck SM, Goldsmith DB *et al.* (2016).
483 Towards quantitative viromics for both double-stranded and single-stranded DNA
484 viruses. *PeerJ* **4**: e2777.
- 485 Roux S, Emerson JB, Eloë-Fadrosch EA, Sullivan MB (2017). Benchmarking viromics: an in
486 silico evaluation of metagenome-enabled estimates of viral community composition and
487 diversity. *PeerJ* **5**: e3817.
- 488 Roux S, Trubl G, Goudeau D, Nath N, Couradeau E, Ahlgren NA *et al.* (2019). Optimizing de
489 novo genome assembly from PCR-amplified metagenomes. *PeerJ* **7**: e6902.
- 490 Sambrook J, Fritsch EF, Maniatis T (1989). *Molecular Cloning: a laboratory manual*. Cold
491 Spring Harbor Laboratory Press: New York.
- 492 Scanlan PD, Buckling A (2012). Co-evolution with lytic phage selects for the mucoid phenotype
493 of *Pseudomonas fluorescens* SBW25. *ISME J* **6**: 1148-1158.
- 494 Schindelin J, Arganda-Carreras I, Frise E, Kaynig V, Longair M, Pietzsch T *et al.* (2012). Fiji: an
495 open-source platform for biological-image analysis. *Nat Methods* **9**: 676-682.
- 496 Silva BSO, Coutinho FH, Gregoracci GB, Leomil L, de Oliveira LS, Froes A *et al.* (2017).
497 Virioplankton Assemblage Structure in the Lower River and Ocean Continuum of the
498 Amazon. *mSphere* **2**.
- 499 Sime-Ngando T (2014). Environmental bacteriophages: viruses of microbes in aquatic
500 ecosystems. *Frontiers in microbiology* **5**: 355-355.
- 501 Simmons M, Bond MC, Drescher K, Bucci V, Nadell CD (2019). Evolutionary dynamics of
502 phage resistance in bacterial biofilms. *bioRxiv*: 552265.
- 503 Skvortsov T, de Leeuwe C, Quinn JP, McGrath JW, Allen CC, McElarney Y *et al.* (2016).
504 Metagenomic Characterisation of the Viral Community of Lough Neagh, the Largest
505 Freshwater Lake in Ireland. *PLoS One* **11**: e0150361.
- 506 Srinivasiah S, Bhavsar J, Thapar K, Liles M, Schoenfeld T, Wommack KE (2008). Phages across
507 the biosphere: contrasts of viruses in soil and aquatic environments. *Research in*
508 *Microbiology* **159**: 349-357.
- 509 Sullivan MB, Weitz JS, Wilhelm S (2017). Viral ecology comes of age. *Environmental*
510 *Microbiology Reports* **9**: 33-35.
- 511 Sutherland IW, Hughes KA, Skillman LC, Tait K (2004). The interaction of phage and biofilms.
512 *FEMS Microbiol Lett* **232**: 1-6.
- 513 Suttle CA (2007). Marine viruses--major players in the global ecosystem. *Nat Rev Microbiol* **5**:
514 801-812.
- 515 Trubl G, Solonenko N, Chittick L, Solonenko SA, Rich VI, Sullivan MB (2016). Optimization of
516 viral resuspension methods for carbon-rich soils along a permafrost thaw gradient. *PeerJ*
517 **4**: e1999.
- 518 Trubl G, Roux S, Solonenko N, Li Y-F, Bolduc B, Rodríguez-Ramos J *et al.* (2019). Towards
519 optimized viral metagenomes for double-stranded and single-stranded DNA viruses from
520 challenging soils. *PeerJ Preprints* **7**: e27640v27641.

- 521 Vega Thurber R, Haynes M, Breitbart M, Wegley L, Rohwer F (2009). Laboratory procedures to
522 generate viral metagenomes. *Nat Protoc* **4**: 470-483.
- 523 Vega Thurber RL, Barott KL, Hall D, Liu H, Rodriguez-Mueller B, Desnues C *et al.* (2008).
524 Metagenomic analysis indicates that stressors induce production of herpes-like viruses in
525 the coral *Porites compressa*. *Proc Natl Acad Sci U S A* **105**: 18413-18418.
- 526 Vidakovic L, Singh PK, Hartmann R, Nadell CD, Drescher K (2017). Dynamic biofilm
527 architecture confers individual and collective mechanisms of viral protection. *Nature*
528 *Microbiology*.
- 529 Weitz JS, Stock CA, Wilhelm SW, Bourouiba L, Coleman ML, Buchan A *et al.* (2015). A
530 multitrophic model to quantify the effects of marine viruses on microbial food webs and
531 ecosystem processes. *ISME J* **9**: 1352-1364.
- 532 Williamson KE, Fuhrmann JJ, Wommack KE, Radosevich M (2017). Viruses in Soil
533 Ecosystems: An Unknown Quantity Within an Unexplored Territory. *Annual Review of*
534 *Virology* **4**: 201-219.
535

Table 1 (on next page)

Sample site and biofilm characteristics.

	VDN	VEV	SNG
Coordinates	46°15'13.5"N	46°30'46.4"N	46°33'23.9"N
	7°06'33.9"E	6°54'43.7"E	6°28'55.3"E
Altitude (m a.s.l.)	1210	766	498
Bacterial abundance [cells m ⁻²]	2.3 x 10 ⁹	1.8 x 10 ¹⁰	4.1 x 10 ¹¹
Chlorophyll-a [μg cm ⁻²]	0.21	0.22	1.21
EPS proteins [μg cm ⁻²]	0.05	0.04	0.24
EPS carbohydrates [μg cm ⁻²]	below detection	below detection	0.08

1

Table 2 (on next page)

Virome dataset statistics

	raw reads		quality trimmed			
	paired-end sequences	GC content (%)	paired-end sequences	GC content (%)	Contigs	Average contig length (bp)
SNG	24 388 096	40.36	24 172 084	40.16	3698	452
VEV	22 459 218	40.51	22 153 818	40.24	11323	645
VDN	23 804 190	40.68	23 422 408	40.21	13591	676

1

Figure 1(on next page)

Overview of methods for the extraction and purification of viruses from stream biofilms.

First, phages are concentrated using either PEG precipitation or TFF. Different physico-chemical extraction procedures were then evaluated for their efficiency. Prior to DNase I digestion, centrifugation and filtration was used to remove cell debris from all samples. Finally, ultracentrifugation in CsCl or sucrose gradients was used to purify viruses for downstream molecular analyses. Combinations of all protocols were evaluated for the recovery of VLPs and DNA yield.

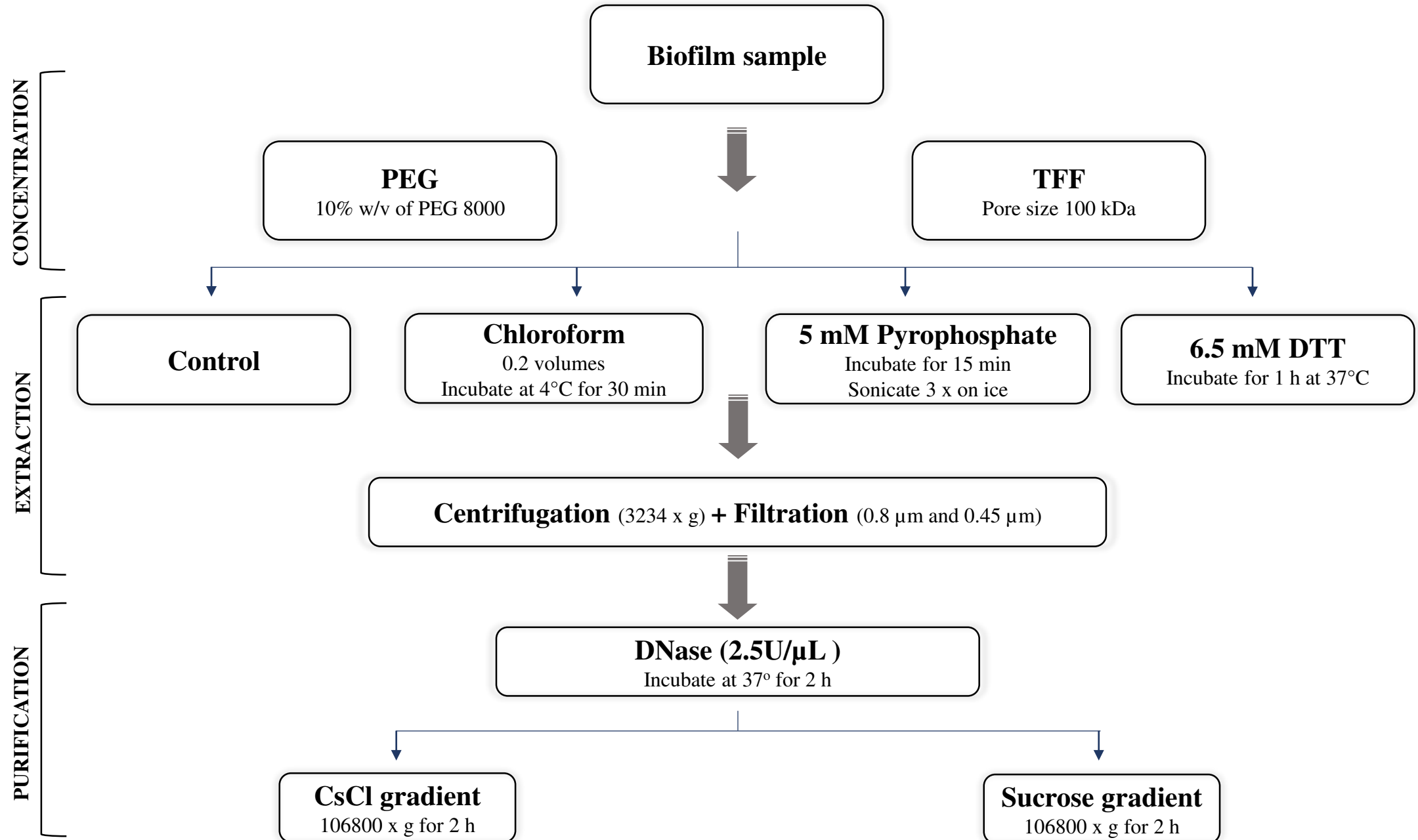


Figure 2

Electron microscopic evidence of virus-like particles in stream biofilm samples.

A large morphological diversity of VLPs, including tailed bacteriophages, lemon-shaped, polyhedral, spherical and filamentous viruses was observed using TEM.

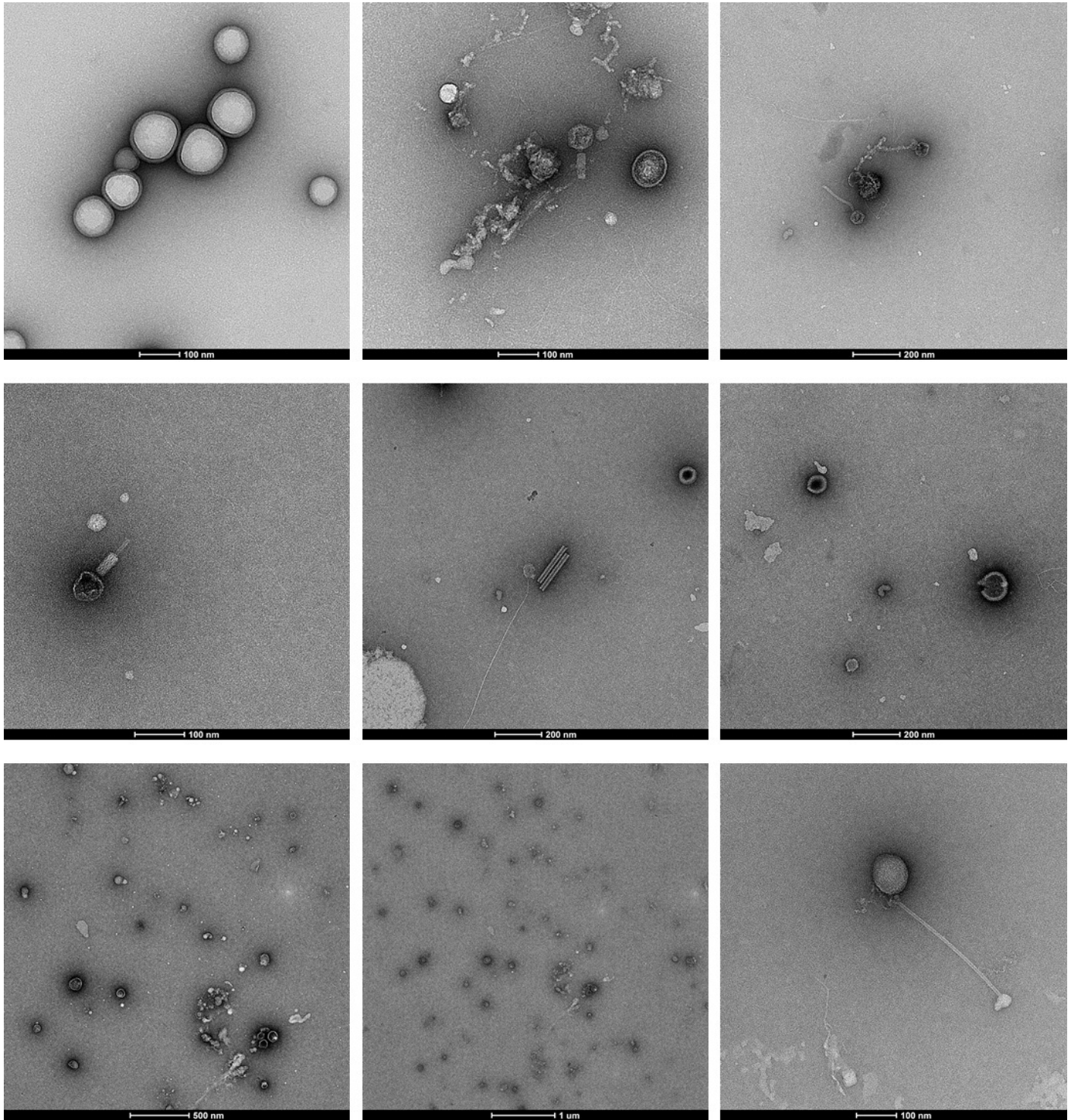
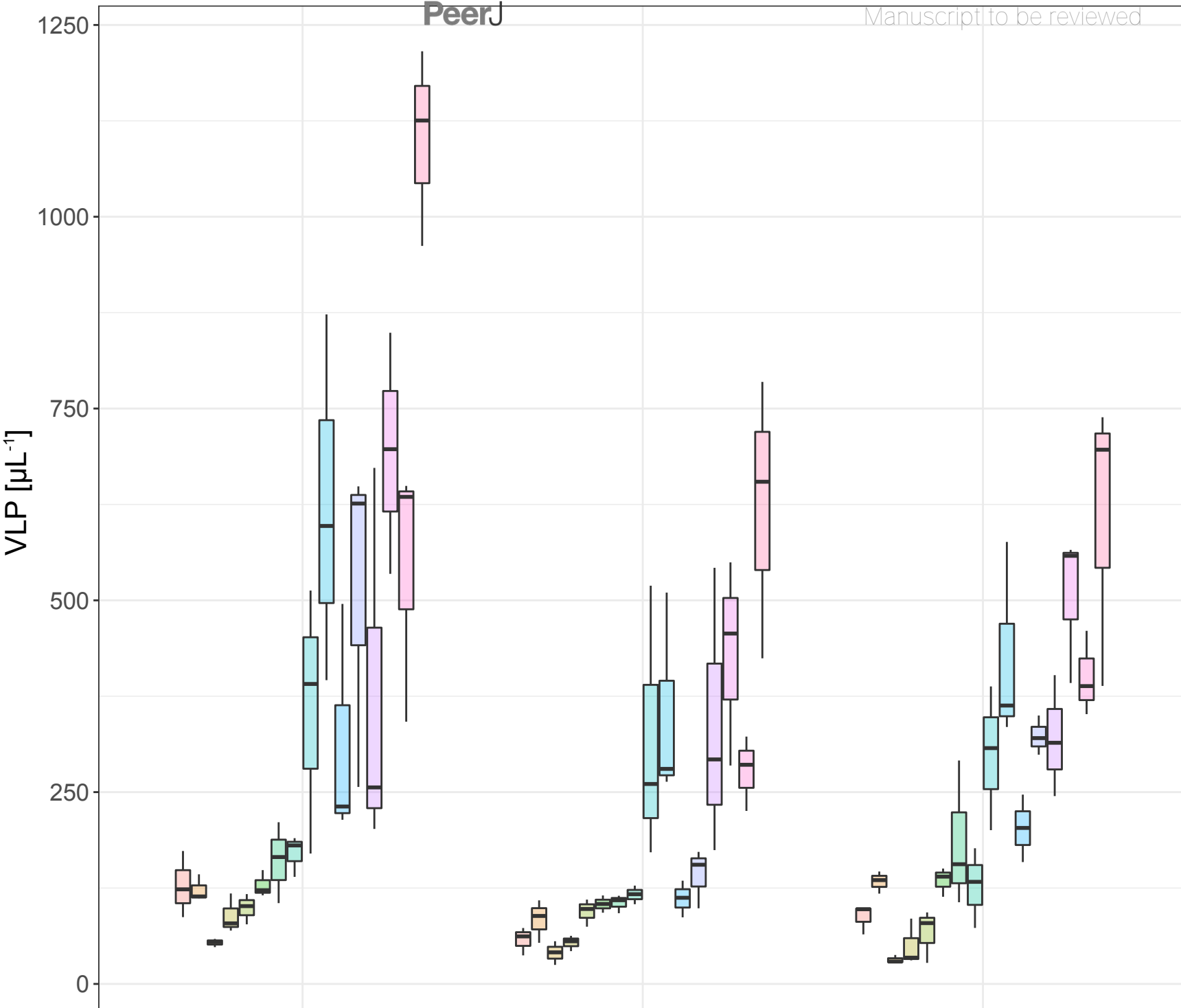


Figure 3(on next page)

VLP yields of the different combination of methods for the extraction and purification of viruses from stream biofilms.

The boxes show the number of VLPs in replicated subsamples processed with each protocol, the median is given as a horizontal line, hinges correspond to the first and third quartile while whiskers extend to the largest and smallest values counted. In each of the three streams tested, a protocol based on TFF, tetrasodium pyrophosphate in combination with sonication and ultracentrifugation in sucrose gradient yielded significantly higher VLP counts than any other combination of protocols.



protocol

- PEG Chloroform CsCl
- PEG Chloroform Sucrose
- PEG Control CsCl
- PEG Control Sucrose
- PEG DTT CsCl
- PEG DTT Sucrose
- PEG Pyrophosphate CsCl
- PEG Pyrophosphate Sucrose
- TFF Chloroform CsCl
- TFF Chloroform Sucrose
- TFF Control CsCl
- TFF Control Sucrose
- TFF DTT CsCl
- TFF DTT Sucrose
- TFF Pyrophosphate CsCl
- TFF Pyrophosphate Sucrose

Figure 4(on next page)

DNA yields from samples processed with different protocols.

None of the protocols involving PEG precipitation resulted in detectable DNA yields (not shown). Protocols using TFF and either no treatment (control), chloroform, DTT, tetrasodium pyrophosphate in combination with sonication for extraction and either CsCl or Sucrose gradient ultracentrifugation for purification yielded between 0.5 and 18.7 ng DNA μL^{-1} . Note that although VLP counts were only 1.8 times higher in the best performing protocol in SNG as compared to the other two samples (VDN, VEV), DNA yields in this sample were more than 14 times higher.

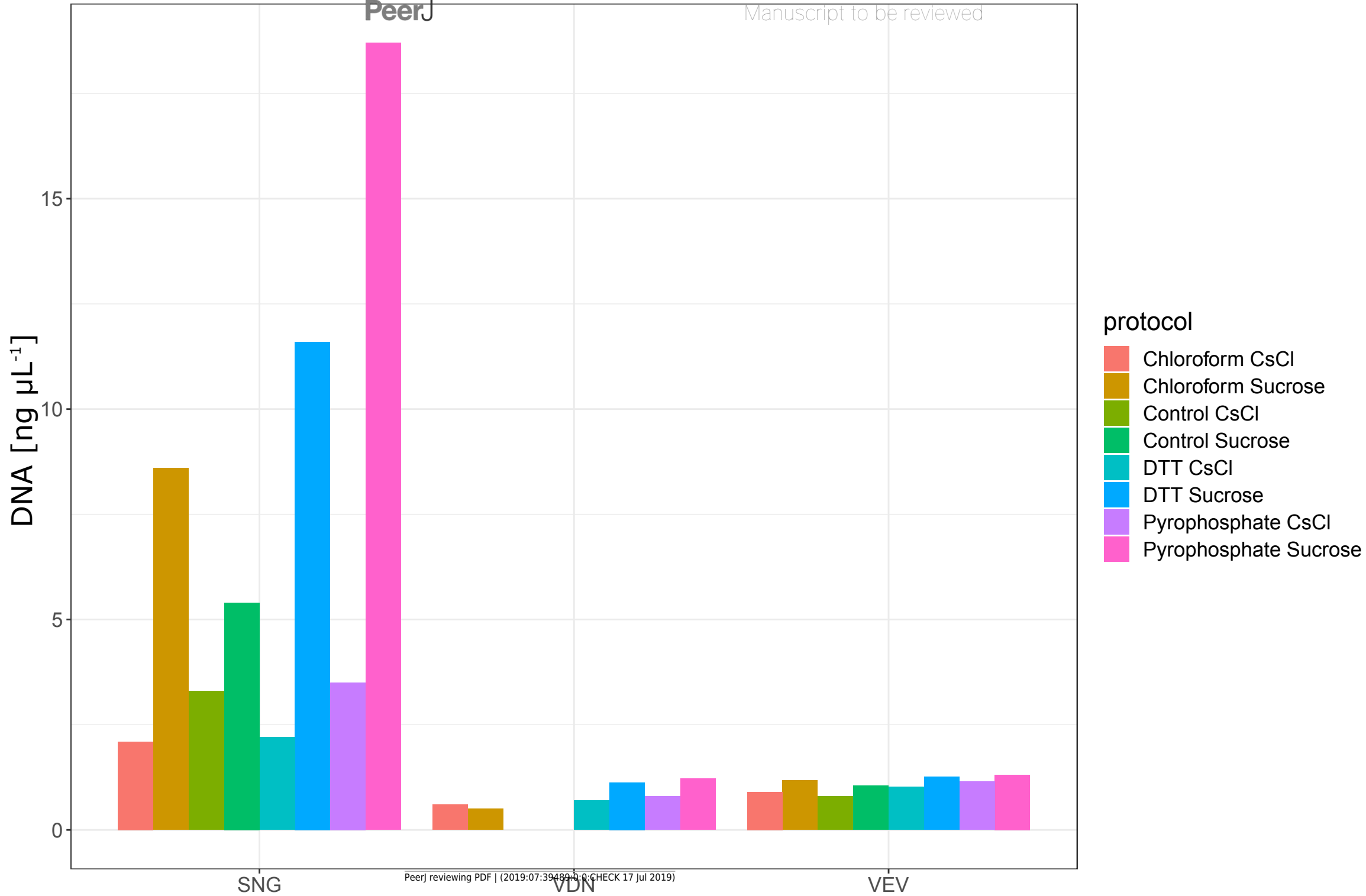


Figure 5(on next page)

Viral contig taxonomic composition.

Taxonomic classification after contig assembly showed that stream biofilm viromes were dominated by not further classified members of Siphoviridae and Myoviridae. The relative composition of contigs was similar among the three samples, however, markedly fewer contigs were obtained from SNG than from the other two stream biofilm samples. ssDNA viruses could not be identified among contigs from any of the streams.

number of contigs

2000

1000

0

SNG

VDN

VEV

taxonomic classification

- Caudovirales
- Cba181virus
- Coopervirus
- Cp220virus
- Kayvirus
- L5virus
- Myoviridae
- other
- P12024virus
- Phicbkvirus
- Podoviridae
- Schizot4virus
- Sep1virus
- Siphoviridae
- T4virus
- Twortvirus
- unclassified bacterial viruses
- unclassified dsDNA phages
- unclassified Lambda-like viruses
- unclassified N4likevirus
- Vequintavirinae

